Materials Science & Engineering A 599 (2014) 134–140

Contents lists available at ScienceDirect

Materials Science & Engineering A

journal homepage: www.elsevier.com/locate/msea

The flow behaviors of CLAM steel at high temperature

Wen-Tao Wang [a], Xun-Zhong Guo [a], Bo Huang [b], Jie Tao [a,*], Hua-Guan Li [a], Wen-Jiao Pei [a]

[a] College of Materials Science and Technology, Nanjing University of Aeronautics and Astronautics, Nanjing 210016, PR China
[b] Institute of Plasma Physics, Chinese Academy of Sciences, Hefei, Anhui 230031, PR China

ARTICLE INFO

Article history:
Received 14 June 2013
Received in revised form
14 January 2014
Accepted 17 January 2014
Available online 24 January 2014

Keywords:
CLAM steel
Hot compression
Flow stress
Constitutive equation

ABSTRACT

The flow behaviors of CLAM steel were investigated to obtain the forming simulation parameters. The hot deformation experiment was performed under the strain rate of 0.001–5 s^{-1} and the temperature of 850–1050 °C on Gleeble-1500 thermo-simulation machine. The results showed that the flow stress decreased with the increasing deformation temperature but increased with the increasing strain rate. Moreover, material constants α, n, ln A and activation energy Q were calculated as a function of strain. Constitutive equation of Arrhenius-type allowing for the effects of strain, strain rate and temperature was developed to describe the hot deformation behaviors of CLAM steel. The flow stress of CLAM steel predicted by the proposed constitutive equation highly coincided with the experimental results, which demonstrated that the developed constitutive equation could precisely predict the flow behaviors of CLAM steel.

© 2014 Elsevier B.V. All rights reserved.

1. Introduction

Compared with nuclear fission energy, nuclear fusion has much more potential owing to its greater energy density and fuel reserves. However, the structural materials for blanket of fusion reactor require high resistance to high-energy neutron irradiation, good thermal conductivity, low thermal expansion coefficient, superior high temperature mechanical properties and good compatibility with the liquid metal. Reduced activation ferritic/martensitic (RAFM) steels have been regarded as candidate structural materials of future fusion power reactors for possessing the outstanding performance mentioned above [1]. Zhou et al. [2] and Hu et al. [3] have investigated the microstructure and mechanical properties of nitride-strengthened RAFM steels. As a kind of RAFM steels, CLAM steel (China low activation martensitic steel) was developed on the basis of F82H, JLF-1, EU ROFER97 and 9Cr-2WVTa to satisfy the application of structural material for blanket of fusion reactor [4]. The mechanical properties such as impact toughness, fatigue properties and fracture toughness [5,6] of CLAM steel were widely researched in the past few years. In addition, the irradiated performance [7], compatibility with the liquid metal LiPb [8,9] and welding performance [10] have also attracted great attention.

Besides those properties mentioned above, the forming properties of CLAM steel also require more concerns. As a good candidate structural material for blanket of fusion reactor, CLAM steel is difficult for cold forming because of high-strength and low plasticity. Hence, hot forming is adopted to fabricate first walls of the blanket or other related products of CLAM steel. It is necessary to obtain the forming properties of CLAM steel at high temperature before real hot forming. The flow stress is an important indicator to evaluate the plastic forming performances of metal materials, determining the applied load and energy consumption in the actual process of plastic deformation. As one of the most frequently-used research methods in metal science, the thermodynamic simulation experiment plays a dominant role in studying flow behaviors of metal materials at high temperature, and the constitutive equation derived from this method can be recognized by professional finite element simulation software, providing a reliable theoretical basis for the numerical simulation and giving a good guidance to the actual forming. The flow behaviors of different alloys, especially aluminum alloys [11,12] and magnesium alloys [13,14] have been adequately investigated at high temperature. In a very recent paper [15], the hot deformation characteristics of a nitride strengthened (NS) martensitic heat resistant steel were studied, including the constitutive equation, the predominant softening processes under different deformation conditions and the corresponding microstructure evolution, etc. However, few analogous researches have been conducted on CLAM steel. Therefore, it is essential to study the hot deformation flow behaviors of CLAM steel. In this study, the hot compression tests were conducted in a wide range of strain rates and temperatures. Then the constitutive equation incorporating flow stress, strain rate, temperature and strain was derived from the true stress–true strain curves. Finally, the precision of the proposed constitutive equation was verified for the entire experimental range.

2. Materials and experimental methods

The chemical composition of CLAM steel used in this investigation is shown in Table 1. CLAM steel specimens were machined to cylinder with the diameter of 10 mm and the height of 15 mm.

* Corresponding author. Fax: +86 25 52112626.
E-mail address: taojie@nuaa.edu.cn (J. Tao).

0921-5093/$ - see front matter © 2014 Elsevier B.V. All rights reserved.
http://dx.doi.org/10.1016/j.msea.2014.01.038

Table 1
Chemical compositions of CLAM steel (wt%).

Cr	W	V	Ta	C	Mn	Fe
9.48	1.48	0.18	0.097	0.098	0.46	Bal

To minimize the friction between the specimens and die during experiments, both ends of the specimen were machined to grooves with depth of 0.2 mm to hold graphite blended with machine oil as the lubricant. The hot compression tests were performed on Gleeble-1500 thermo-simulation machine in the temperature range from 850 to 1050 °C with an interval of 50 °C under the strain rates of 0.001, 0.01, 0.1, 1 and 5 s^{-1}. The specimens were heated to deformation temperature at a heating rate of 10 °C s^{-1}, and then maintained at that temperature for 300 s to homogenize the temperature before compression. Finally the specimens were quenched in water immediately after compression. The maximum height reduction was 60% for all the specimens of compression tests.

3. Results and discussion

3.1. Analysis of flow behaviors

True stress–true strain curves of CLAM steel could be achieved by the conversion of load–displacement curves that were directly recorded by the computer. Fig. 1 shows the true stress–true strain curves of CLAM steel obtained from the experiments.

It can be seen in Fig. 1 that the stress rapidly increases first and then slows down until reaching a steady state with the increment of strain. During the deformation process at elevated temperature, the dynamic softening and work hardening function simultaneously. At the very start of the deformation, the dislocation sources start, thus dramatically increasing the dislocation density, inhibiting the motion of dislocations owing to the interaction of dislocations. Therefore, the effects of work hardening exceeds that of the dynamic softening, leading to the rapid increase of stress. However, work hardening effect is gradually compensated by the softening from recovery and recrystallization at further deformation, which can explain the behaviors of the rest part but the initial sharply rising stage of the true stress–true strain curves.

Fig. 1 also reveals that the deformation temperature and strain rate have a great influence on the flow stress. Under the same strain rate, the flow stress level decreases with the increasing deformation temperature. According to the main softening mechanism of metals, it can be explained by a combined effect of two factors. The one is dynamic recovery and recrystallization occurred at high temperature. The other factor is the reduction of critical shear stress induced by elevating temperature, which enhances the average kinetic energy of atoms as well as the mobility of point defects and dislocations.

Furthermore, at the same deformation temperature, the flow stress is positively influenced by the increase of the strain rate, which can be attributed to the inadequacy of plastic deformation. On the contrary, the elastic deformation plays a prominent role among the total deformation. Hence, the following obvious work hardening behavior results in the increment of flow stress. In addition, no sufficient time is left for dynamic recovery and recrystallization under higher strain rates, which weakens the softening effect and consequently raises the flow stress level.

3.2. Constitutive equation of flow behavior

The combined effects of the temperature and strain rate on the deformation behavior can be represented by the Zener–Hollomon parameter (Z) in an exponential-type equation [16] as follows:

$$Z = \dot{\varepsilon}\exp\left(\frac{Q}{RT}\right) \tag{1}$$

where R is the universal gas constant (8.314 J mol^{-1} K^{-1}); T is the absolute temperature (K); Q is the activation energy (J mol^{-1}) and $\dot{\varepsilon}$ is the strain rate (s^{-1}). Z parameter is strain rate factor for temperature compensation.

Sellars and McTegart [17] proposed a constitutive equation containing the deformation activation energy Q and temperature T, to describe the relationship between strain rate, temperature and flow stress, especially at high temperature. The equation is mathematically expressed as follows:

$$\dot{\varepsilon} = AF(\sigma)\exp\left(\frac{-Q}{RT}\right) \tag{2}$$

where $F(\sigma)$ is the function of stress. It is divided into three forms of expression below in terms of stress level.

$$F(\sigma)\begin{cases}\sigma^{n'} & \alpha\sigma < 0.8\\ \exp(\beta\sigma) & \alpha\sigma > 1.2\\ [\sinh(\alpha\sigma)]^{n} & \text{for all } \sigma\end{cases} \tag{3}$$

where A, α, β, n' and n are the materials constants, $\alpha=\beta/n'$.

Many research results [18–21] showed that the combination of Eqs. (2) and (3) could well describe the hot deformation behavior of metallic materials under a certain strain, even though the influence of strain was ignored. However, recent researches [22–24] demonstrated that the strain had great effects on materials constants Q, α, n and A. To study the mathematical relationships between the strain ε and materials constants (Q, α, n and A), the values of Q, α, n and A under different strains were evaluated first and then fitted by least square method. Herein, we take true strain of 0.4 as an example to explain the process to acquire the values of Q, α, n and A.

The correlations between strain rate and stress at the low stress level ($\alpha\sigma < 0.8$) and high stress level ($\alpha\sigma > 1.2$) are given as below:

$$\dot{\varepsilon} = A\sigma^{n'}\exp\left(\frac{-Q}{RT}\right) = B\sigma^{n'} \tag{4}$$

$$\dot{\varepsilon} = A\exp(\beta\sigma)\exp\left(\frac{-Q}{RT}\right) = B'\exp(\beta\sigma) \tag{5}$$

where B and B' are the material constants.

Eqs. (6) and (7) are derived by taking the logarithm of both sides of Eqs. (4) and (5).

$$\ln\dot{\varepsilon} = n'\ln\sigma + \ln B \tag{6}$$

$$\ln\dot{\varepsilon} = \beta\sigma + \ln B' \tag{7}$$

The relevance between the flow stress and the strain rate under a certain temperature can be evaluated by substituting the values of the flow stress and corresponding strain rate under the strain of 0.4 into Eqs. (6) and (7). It is obviously seen in Fig. 2 that the relationships between the flow stress and the strain rate can be approximately expressed as straight lines, which are supposed to be parallel to each other under different temperatures according to Eqs. (6) and (7). The values of n' and β could be gained at each temperature by linear fitting the slope of the lines in $\ln\dot{\varepsilon}-\ln\sigma$ and $\ln\dot{\varepsilon}-\sigma$ plots, respectively. The mean values of β and n' can be computed as $\beta=0.0552\pm0.0039$ MPa^{-1}, $n'=7.99\pm1.53$ and $\alpha=\beta/n'=0.0069\pm0.0017$ MPa^{-1}. The coefficient of determination (R^2) is used to evaluate the degree of fitting of each linear regression, as is shown in Fig. 2. The results demonstrate the high accuracy and reliability of the linear regression. A different method was used to determine the α value in reference [15],

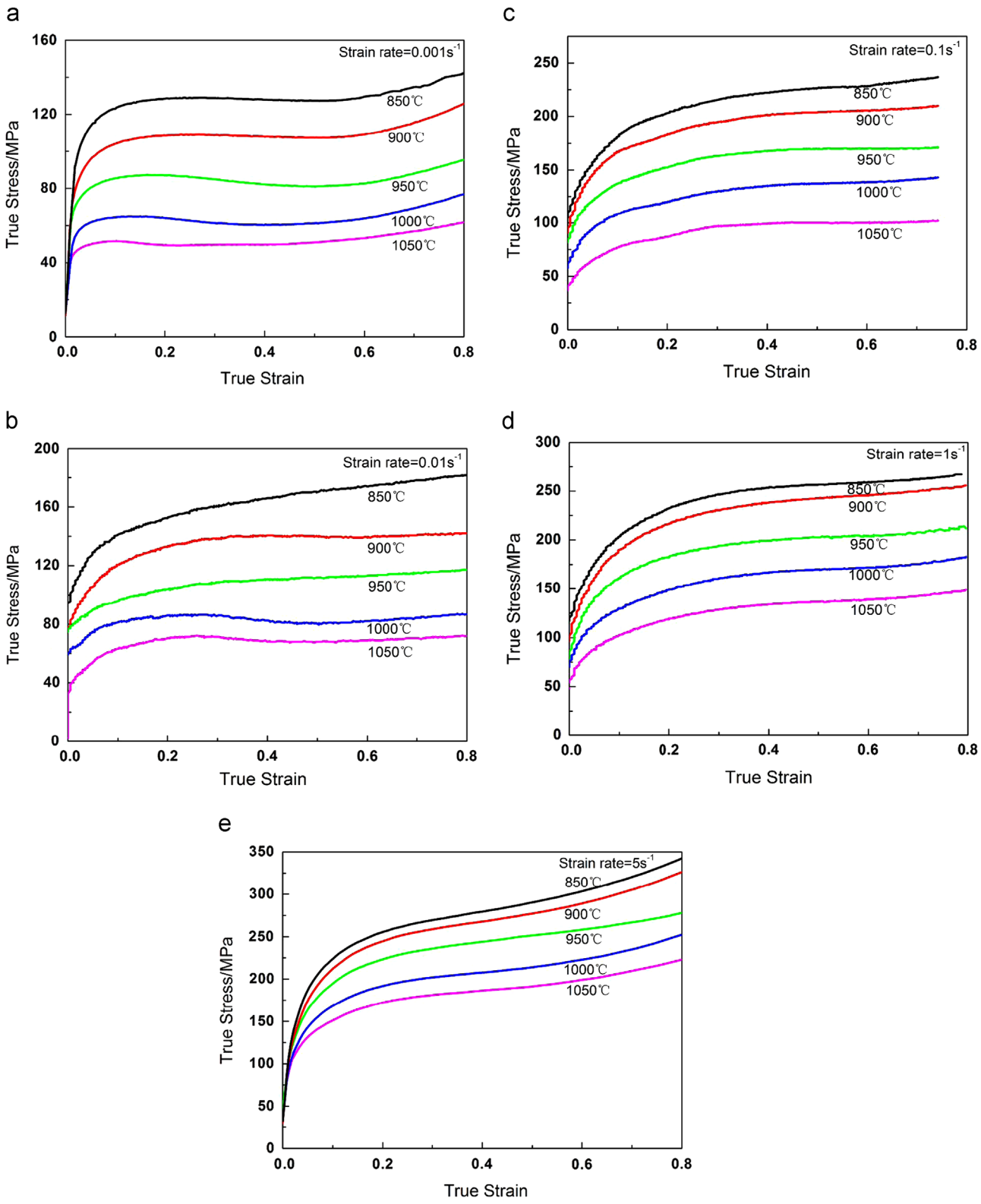

Fig. 1. True stress–true strain curves for CLAM steel under different deformation conditions: (a) 0.001 s^{-1}; (b) 0.01 s^{-1}; (c) 0.1 s^{-1}; (d) 1 s^{-1}; and (e) 5 s^{-1}.

that is firstly fixing the α value to a constant, and the following steps were the same as below.

For both low and high stress levels, Eq. (2) can be transformed to the following form:

$$\dot{\varepsilon} = A[\sinh(\alpha\sigma)]^n \exp\left(\frac{-Q}{RT}\right) \tag{8}$$

Taking the logarithm of both sides of Eq. (8), we can derive the following equation

$$\ln[\sinh(\alpha\sigma)] = \ln\dot{\varepsilon}/n + Q/(nRT) - \ln A/n \tag{9}$$

The relationships between $\ln\dot{\varepsilon}$ and $\ln[\sinh(\alpha\sigma)]$ can be acquired by substituting strain rate values and flow stress values under the strain of 0.4 at each temperature into Eq. (9), as is shown in Fig. 3.

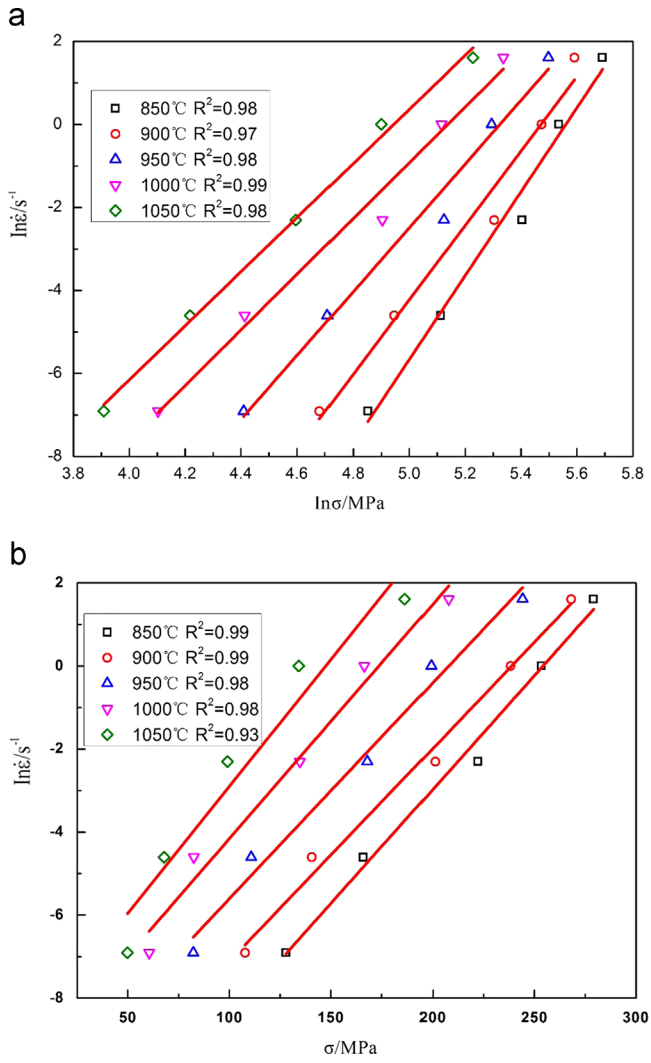

Fig. 2. Relationships between strain rate and stress at different deformation temperatures: (a) relationships between $\ln\sigma$ and $\ln\dot{\varepsilon}$; and (b) relationships between σ and $\ln\dot{\varepsilon}$.

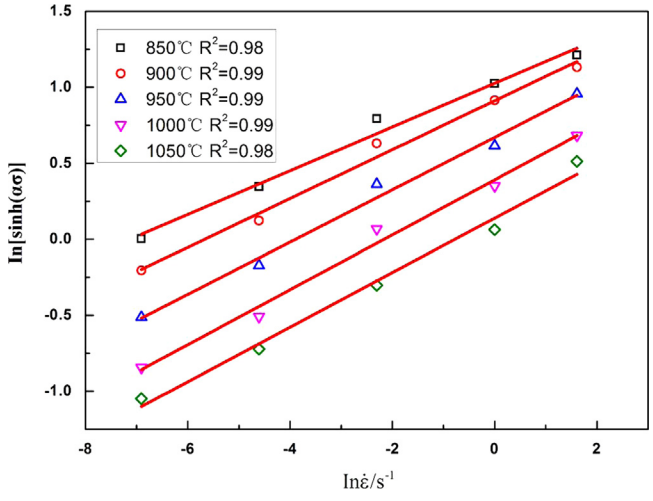

Fig. 3. Relationships between $\ln[\sinh(\alpha\sigma)]$ and strain rate $\dot{\varepsilon}$ at different deformation temperatures.

The value of the material constant n, presenting as the reciprocal of slope values of the lines in Fig. 3, can be evaluated as 6.02 ± 0.59 by arithmetic averaging those slope values. Judging by the coefficient of determination (R^2) of each linear fitting, the regression lines have good statistical significance.

For a certain strain rate, Eq. (10) could be derived by differentiating Eq. (9)

$$Q = Rnd\{\ln[\sinh(\alpha\sigma)]\}/d(1/T) \tag{10}$$

Therefore, the value of Q can be acquired by substituting the values of related parameters into Eq. (10). Among these parameters, R is the gas constant and n can be calculated by Eq. (9). $d\{\ln[\sinh(\alpha\sigma)]\}/d(1/T)$ is the slope value of each line which describes the relationship between $\ln[\sinh(\alpha\sigma)]$ and $1/T$, and the coefficient of determination (R^2) of each line is also evaluated, as is shown in Fig. 4. Consequently, it is easy to evaluate the value of activated energy (Q) as 372.62 ± 58.81 kJ/mol by arithmetic averaging the values of Q derived from Eq. (10) at different strain rates.

Combining Eq. (9) with the previously obtained Q and n, the value of material constant A is calculated as $(1.87 \pm 0.43) \times 10^{14}\ s^{-1}$.

It is found that the errors of the results are a little larger than those of reference [15]. The only difference in calculating the value of α, n, A and Q between the two papers is how to determine the α value. Therefore, it can be concluded that the error of α value results in the errors of other material constants.

To establish a constitutive equation that could precisely describe the flow behaviors of CLAM steel, the strain compensation is taken into consideration in this work. The values of material constants (i.e. α, Q, n, A) of the constitutive equation are calculated under different strains in a practical range from 0.05 to 0.75 with the interval of 0.05 by the same method used above. Then, polynomial fitting is carried out on these material constants and the strain with the order varying from 2 to 9 to get the relationships between them. The results show that a fifth order polynomial fitting, as shown in Eq. (11), could represent these relationships with high accuracy (Fig. 5). The polynomial fitting coefficients are given in Table 2.

$$\begin{cases} \alpha = B_0 + B_1\varepsilon + B_2\varepsilon^2 + B_3\varepsilon^3 + B_4\varepsilon^4 + B_5\varepsilon^5 \\ n = C_0 + C_1\varepsilon + C_2\varepsilon^2 + C_3\varepsilon^3 + C_4\varepsilon^4 + C_5\varepsilon^5 \\ Q = D_0 + D_1\varepsilon + D_2\varepsilon^2 + D_3\varepsilon^3 + D_4\varepsilon^4 + D_5\varepsilon^5 \\ \ln A = E_0 + E_1\varepsilon + E_2\varepsilon^2 + E_3\varepsilon^3 + E_4\varepsilon^4 + E_5\varepsilon^5 \end{cases} \tag{11}$$

Up to now, all the relevant materials constants (i.e. α, Q, n, A) have been evaluated. The constitutive equation to describe the hot deformation flow behaviors of CLAM steel can be obtained by substituting these materials constants into Eq. (8).

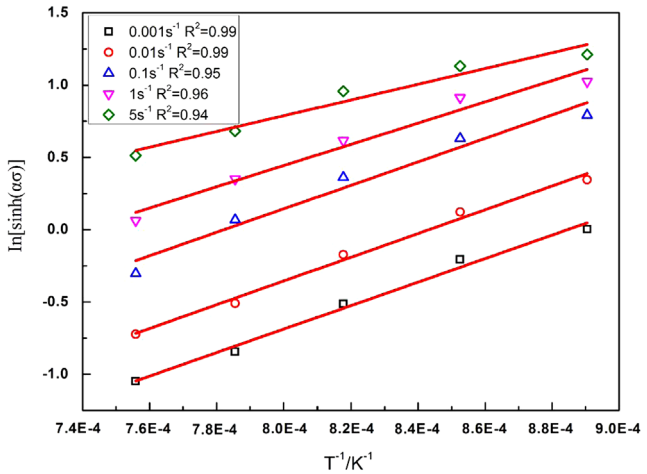

Fig. 4. Relationships between $\ln[\sinh(\alpha\sigma)]$ and temperature at different strain rates.

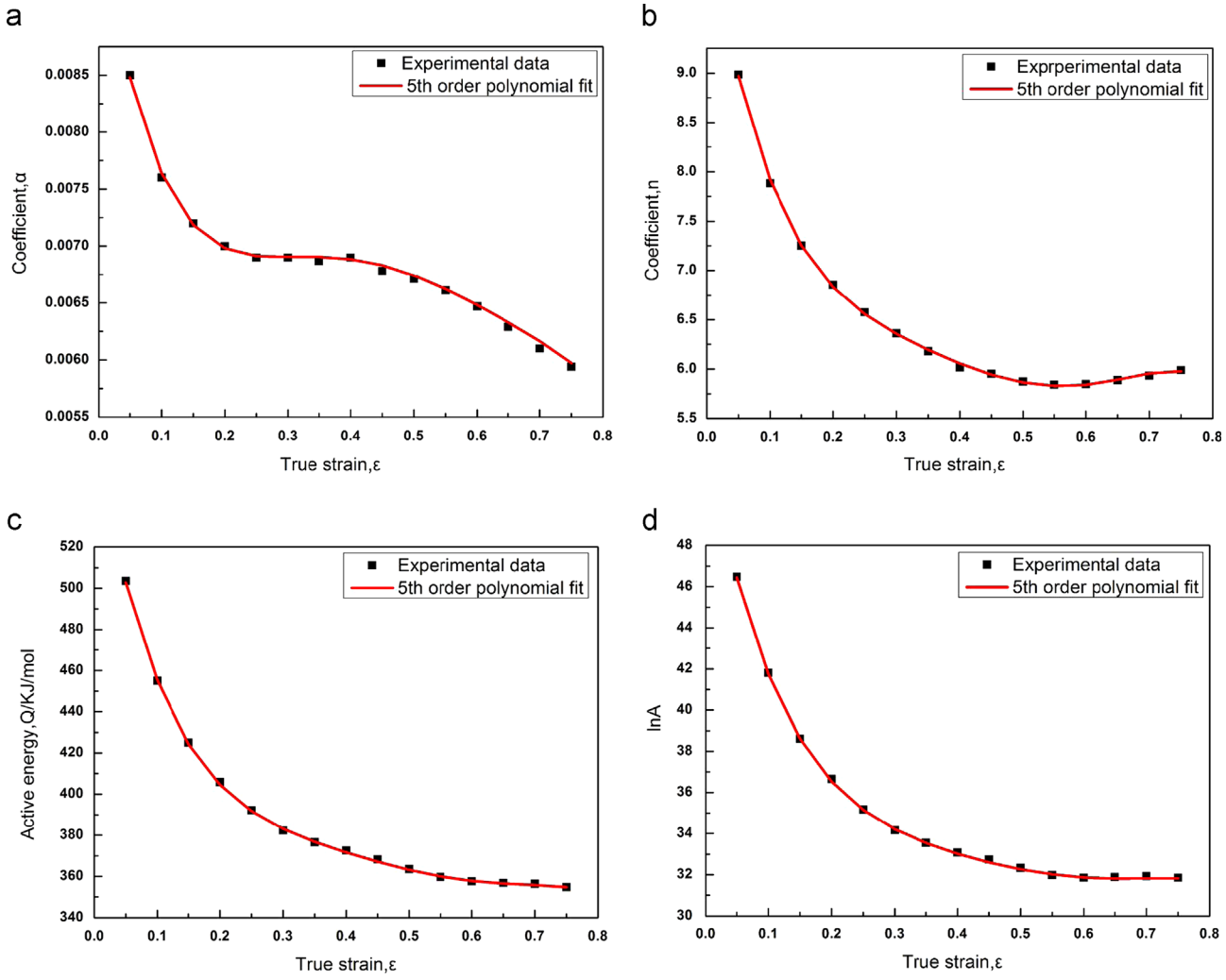

Fig. 5. Relationships between: (a) α; (b) n; (c) Q; and (d) ln A and true strain by polynomial fit of CLAM steel.

Table 2
Polynomial fitting results of Q, α, n and A of CLAM steel.

α		n		Q		ln A	
B_0	0.0099	C_0	10.601	D_0	574	E_0	53.3
B_1	−0.0356	C_1	−40.041	D_1	−1715	E_1	−163.5
B_2	0.1605	C_2	165.386	D_2	6451	E_2	582.4
B_3	−0.3391	C_3	−373.976	D_3	−12,971	E_3	−1124.7
B_4	0.3338	C_4	423.010	D_4	13,058	E_4	1105.8
B_5	−0.1267	C_5	−184.131	D_5	−5146	E_5	−429.2

3.3. Verification of the constitutive equation

Stress values of random temperature and strain could be calculated with the developed constitutive equation. The precision of the constitutive equations could be evaluated by comparing these calculated values with experimental values, as is shown in Fig. 6. It is found out that the proposed constitutive equation gives an accurate estimation of the flow stress for CLAM steel in most of the experimental conditions involved in this work. However, obvious differences between experimental and predicted flow stresses can be observed under the circumstances that the temperature is 850 °C and the strain rates are 1 s^{-1} and 5 s^{-1}. The potential reason is that there is less time for the heat produced by deformation to transfer under high strain rates compared with that of lower strain rates, thus leading to a significant part of flow softening [25]. It may be controversial here that such phenomenon is also supposed to occur at other temperatures under the strain rates of 1 s^{-1} and 5 s^{-1}. It is likely that the influence of the heat generating from deformation on flow softening is not so significant at temperatures higher than 850 °C, because the actual experimental temperature can provide enough energy to induce flow softening [26]. More detailed evidences remain to be further investigated.

The correlation coefficient (R) and average absolute relative error (AARE) are applied here to quantitatively evaluate the precision of the established constitutive equation. Their expressions are as follows:

$$r = \frac{\sum_{i=1}^{N}(E_i-\overline{E})(P_i-\overline{P})}{[\sum_{i=1}^{N}(E_i-\overline{E})^2\sum_{i=1}^{N}(P_i-\overline{P})^2]^{1/2}} \tag{12}$$

$$AARE(\%) = \frac{1}{N}\sum_{i=1}^{N}\left|\frac{E_i-P_i}{E_i}\right| \times 100 \tag{13}$$

where E_i is the experimental value and P_i is the calculated value acquired from the constitutive equation. $\overline{E}$ and $\overline{P}$ are the average values of E_i and P_i, respectively. N is the number of data employed

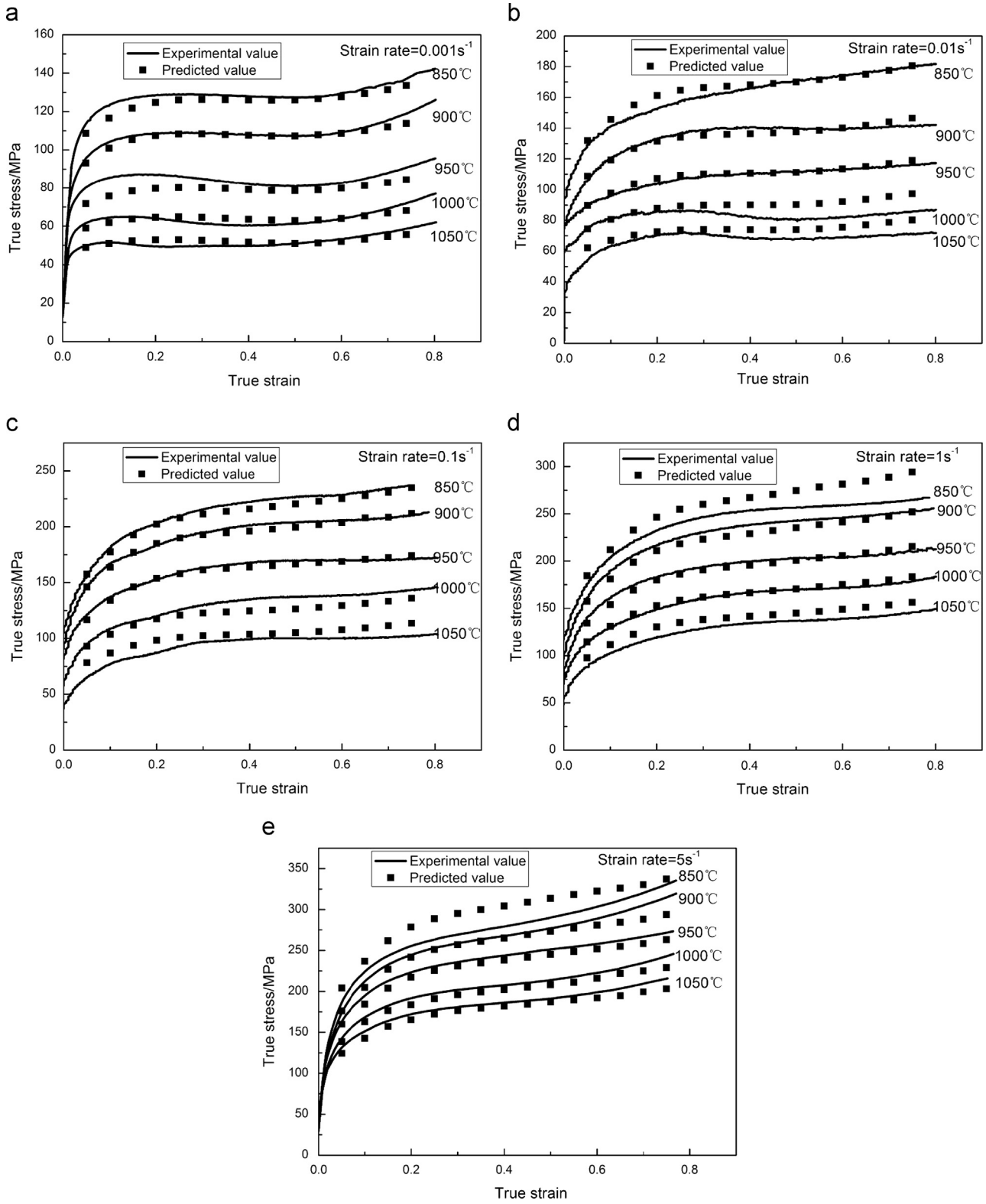

Fig. 6. Comparison between experimental values and calculation values for flow stress at different strain rates: (a) 0.001 s^{-1}; (b) 0.01 s^{-1}; (c) 0.1 s^{-1}; (d) 1 s^{-1}; and (e) 5 s^{-1}.

in the investigation. The correlation coefficient is a commonly used statistical parameter, providing information about the strength of linear relationship between the experimental and the calculated values. AARE is computed through a term-by-term comparison of the relative error and therefore is an unbiased statistical parameter for measuring the predictability of a model/equation [26,27].

As is shown in Fig. 7, the correlation coefficient between experimental and predicted data is 0.993, which suggests the applicability of constitutive equations from one aspect. On the

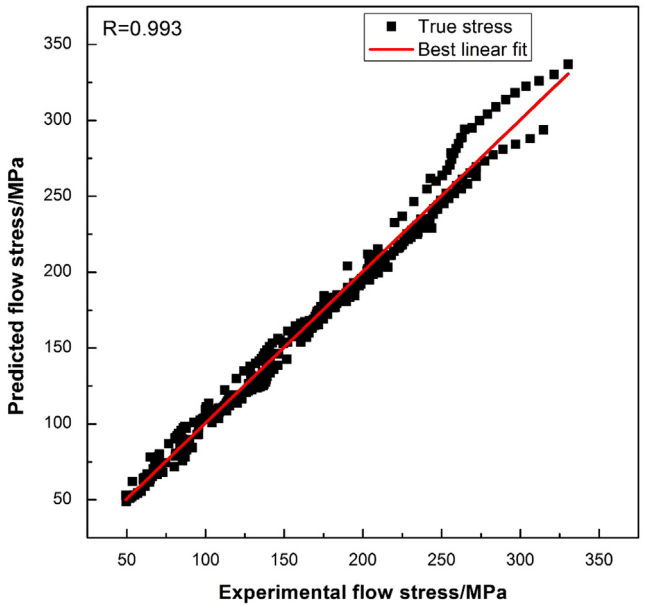

Fig. 7. Correlations between experimental and predicted flow stress at different deformation conditions.

other hand, the average absolute relative error is as low as 3.90%. Both results demonstrate that the developed constitutive equations could predict the hot deformation flow behaviors in good accuracy.

4. Conclusions

(1) The true stress–true strain curves obtained during hot compression of CLAM steel exhibited that the values of true stress rose rapidly and then slowly increased to a steady state, which was the combined function of dynamic softening and work hardening.
(2) The deformation temperature and strain rate had great effects on the flow stress of CLAM steel, manifesting that the flow stress increased with the growing of the strain rate but varied inversely with the deformation temperature.
(3) The relationships between material constants (i.e. α, A, n, and Q) and the strain were gained through a fifth order polynomial fitting. Then a constitutive equation incorporating the influence of strain was established based on the above results.
(4) It was revealed that the proposed constitutive equations could well predict the flow stress in the given ranges of the experimental temperatures and strain rates based on the comparison between the experimental and calculated values.

Acknowledgments

The present work has been supported by the National Natural Science Foundation of China (No. 51205196), the Doctoral Foundation of Ministry of Education of China (No. 20123218120029) and the special foundations for significant achievements of Jiangsu Province of China (No. BA2012124). The authors would like to thank FDS group of Institute of Plasma Physics, Chinese Academy of Sciences and Jiangsu Huayang Metal Pipes Company Ltd. for providing the CLAM tube blank and their facilities.

References

[1] W. Sha, Steels: From Materials Science to Structural Engineering, Springer, London, 2013.
[2] Q.G. Zhou, W.F. Zhang, W. Yan, W. Wang, W. Sha, Y.Y. Shan, K. Yang, Metall. Mater. Trans. A 43 (2012) 5079–5087.
[3] P. Hu, W. Yan, L.F. Deng, W. Sha, Y.Y. Shan, K. Yang, Fusion Eng. Des. 85 (2010) 1632–1637.
[4] J.N. Yu, Q.Y. Huang, F.R. Wan, J. Nucl. Mater. 367–370 (2007) 97–101.
[5] Y. Li, Q. Huang, Y. Wu, T. Nagasaka, T. Muroga, J. Nucl. Mater. 367–370 (2007) 117–121.
[6] Y.F. Li, T. Nagasaka, T. Muroga, Q.Y. Huang, Y.C. Wu, J. Nucl. Mater. 386–388 (2009) 495–498.
[7] L. Peng, Q.Y. Huang, C.J. Li, S.J. Liu, J. Nucl. Mater. 386–388 (2009) 312–314.
[8] Z. Zhu, M. Zhang, S. Gao, Y. Song, C. Li, L. Peng, Z. Guo, Y. Wang, S. Liu, M. Kong, Q. Huang, Fusion Eng. Des. 84 (2009) 5–8.
[9] Y.P. Chen, Q.Y. Huang, S. Gao, Z.Q. Zhu, X.Z. Ling, Y. Song, Y.L. Chen, W.H. Wang, Fusion Eng. Des. 85 (2010) 1909–1912.
[10] Q.Y. Huang, C.J. Li, Q.S. Wu, S.J. Liu, S. Gao, Z.H. Guo, Z.L. Yan, B. Huang, Y. Song, Z.Q. Zhu, Y.P. Chen, X.H. Ling, Y.C. Wu, J. Nucl. Mater. 417 (2011) 85–88.
[11] X.D. Huang, H. Zhang, Y. Han, W.X. Wu, J.H. Chen, Mater. Sci. Eng. A 527 (2010) 485–490.
[12] Y. Deng, Z.M. Yin, J.W. Huang, Mater. Sci. Eng. A 528 (2011) 1780–1786.
[13] Y.J. Qin, Q.L. Pan, Y.B. He, W.B. Li, X.Y. Liu, X. Fan, Mater. Sci. Eng. A 527 (2010) 2790–2797.
[14] O. Sabokpa, A. Zarei-Hanzaki, H.R. Abedi, N. Haghdadi, Mater. Des. 39 (2012) 390–396.
[15] W.F. Zhang, X.L. Li, W. Sha, W. Yan, W. Wang, Y.Y. Shan, K. Yang, Mater. Sci. Eng. A 590 (2014) 199–208.
[16] C. Zener, H. Hollomon, J. Appl. Phys. 15 (1944) 22–27.
[17] C.M. Sellars, W.J. McTegart, Acta Metall. 14 (1966) 1136–1138.
[18] S. Banerjee, P.S. Robi, A. Srinivasan, L.P. Kumar, Mater. Sci. Eng. A 527 (2010) 2498–2503.
[19] Y.H. Xiao, C. Guo, Mater. Sci. Eng. A 528 (2011) 5081–5087.
[20] M.R. Rokni, A. Zarei-Hanzaki, A.A. Roostaei, A. Abolhasani, Mater. Des. 32 (2011) 4955–4960.
[21] H. Mirzadeh, J.M. Cabrera, J.M. Prado, A. Najafizadeh, Mater. Sci. Eng. A 528 (2011) 3876–3882.
[22] Y.C. Lin, M.S. Chen, J. Zhong, Comput. Mater. Sci. 42 (2008) 470–477.
[23] Y.C. Lin, Y.C. Xia, X.M. Chen, M.S. Chen, Comput. Mater. Sci. 50 (2010) 227–233.
[24] H.Y. Li, D.D. Wei, J.D. Hu, Y.H. Li, S.L. Chen, Comput. Mater. Sci. 53 (2012) 425–430.
[25] Y.C. Lin, M.S. Chen, J. Zhong, Mech. Res. Commun. 35 (2008) 142–150.
[26] S. Mandal, V. Rakesh, P.V. Sivaprasad, S. Venugopal, K.V. Kasiviswanathan, Mater. Sci. Eng. A 500 (2009) 114–121.
[27] N. Haghdadi, A. Zarei-Hanzaki, H.R. Abedi, Mater. Sci. Eng. A 535 (2012) 252–257.